#466

FERMILAB-PUB-80-114-E
Submitted to Physical Review C

Differential Ranges of Sc Fragments from the Interaction of ^{238}U with 0.8-400 GeV Protons

D.R. Fortney* and N.T. Porile

Department of Chemistry, Purdue University,
W. Lafayette, Indiana 47907

Differential ranges of $^{44}Sc^{m}$, ^{46}Sc, ^{47}Sc, and ^{48}Sc emitted at 90° to the beam in the interaction of ^{238}U with 0.8, 3.0, 11.5, and 400 GeV protons have been measured and transformed to the corresponding energy spectra. The mean fragment energies decrease from 83±5 to 58±4 MeV between 0.8 and 11.5 GeV and to 50±3 MeV at 400 GeV. The widths of the spectra increase markedly with energy up to 11.5 GeV and more slowly thereafter. Isotopic differences are minor although the spectra of neutron-deficient $^{44}Sc^{m}$ are somewhat broader, particularly at 0.8 GeV. The results are compared with the statistical fragment emission model and discussed in terms of asymmetric binary fission and deep spallation mechanisms.

NUCLEAR REACTIONS $^{238}U(p,x)^{44}Sc^{m}$, ^{46}Sc, ^{47}Sc, ^{48}Sc. T_p = 0.8, 3.0, 11.5, 400 GeV. Measured differential ranges at 90°; deduced energy spectra.

*Present address: Sandia Corporation, Albuquerque, New Mexico

I. Introduction

The formation of scandium nuclides in the interaction of ^{238}U with protons is the result of highly inelastic interactions occurring at high energies. The excitation functions for the formation of these nuclides thus rise steeply with proton energy up to $\sim$ 10 GeV[1] indicating that high bombarding energies are necessary. The forward-to-backward emission ratios (F/B) measured in thick-target experiments also increase with bombarding energy up to 3 GeV.[1] An analysis of these results in terms of the conventional two-step model of high-energy reactions indicates that the formation of Sc nuclides is the result of processes in which excitation energies as high as 1 GeV are transferred to the struck nucleus in the initial interaction. Above 3 GeV the F/B ratios decrease with increasing proton energy in a similar way as the F/B of light fragments and deep spallation products.[2,3] However, the results for Sc are rather unique in that the F/B values measured at 300 GeV, the highest energy at which the reaction was studied, are as low as unity, indicating essentially no forward momentum transfer. The only other products of highly inelastic interactions known to have such low F/B are some nuclides in the A=45-65 mass region formed in the interaction of gold with 300 GeV protons.[4]

The ranges of the scandium nuclides also exhibit a substantial variation with bombarding energy.[1] A rapid decrease in range was thus noted between 0.8 and 10 GeV, followed by a slower decrease between 10 and 300 GeV. The momenta of Sc fragments at 0.8 GeV were found to be consistent with the fission of ^{203}Bi on the basis of liquid drop model calculations.[5] The need to postulate such a light fissioning nucleus

is again indicative of the high excitation energies needed to produce Sc nuclides.

It is thus apparent that the study of the emission of Sc and similar fragments in the interaction of high-energy protons with heavy elements may be used to probe nuclear matter under fairly extreme conditions. Furthermore, the peak in the F/B ratio observed at 3 GeV and the concomitant changes in the angular distribution from forward to sideward-peaked[6] have been related[7] to the changes in the nature of the interaction of hadrons with nuclei at ultra-relativistic energies.[8] It has thus been pointed out[9,10] that due to relativistic effects a high-energy proton may interact collectively with a part of the nucleus instead of with the individual target nucleons, as at lower energies. This is particularly true in central collisions with heavy elements, where a significant number of nucleons lie in the path of the incident proton. Since the Sc nuclides are formed in just these collisions they can be used to probe this important new mechanism.

While our previous excitation function measurements and thick-target recoil studies of the formation of Sc fragments in the interaction of ^{238}U with 1-300 GeV protons[1] provided some interesting results, these experiments are necessarily limited in the type of information that is obtainable. We present here the results of more detailed experiments, namely, differential range measurements performed on Sc nuclides emitted in the interaction of ^{238}U with 0.8-400 GeV protons. As pointed out in previous studies of this type,[11,12] the shape of the spectrum is of value in probing the details of the reaction mechanism. The abovementioned decrease in the mean range of scandium isotopes could thus be the

result of an increasing contribution of a low-energy component, a shift of the entire spectrum towards lower energies, etc. It is obvious that these various possibilities place different constraints on the reaction mechanism.

With the aid of appropriate range-energy relations, the differential ranges may be converted to energy spectra. While the spectra obtained in this fashion are of rather low resolution when compared to those determined directly, they do offer some unique advantages. Perfect elemental and isotopic resolution are thus obtained. In addition, the spectra do not have a significant low-energy cutoff and virtually the entire spectrum is measurable. By contrast, counter measurements have a cutoff imposed by the thickness of the ΔE detector and, for fragments as massive as Sc, this cutoff can be high enough to preclude a determination of the peak in the spectrum. There have been many measurements of the energy spectra of fragments emitted in high-energy proton reactions. A survey may be found in Ref. 13. Of particular relevance to our work are the experiments of Poskanzer and collaborators,[13,14] who measured the spectra of He-Ar fragments emitted in the interaction of uranium with 5 GeV protons. These workers developed a statistical model for the emission of fragments from highly excited nuclei which may be applied to the scandium data. For the very lightest fragments,e.g. He and Li, these workers also found a significant difference in the spectral shapes of neutron-deficient and neutron-excess isotopes, the former having harder spectra. While the origin of this difference is not completely clear, it appears to be consistent with the predictions of the coalescence and

fireball models.[15] Since counter techniques have not as yet yielded spectra of isotopically resolved fragments in the mass range of present interest, it is not clear whether such differences persist for Sc fragments. The present study addresses itself to this question; data are presented for four Sc nuclides ranging from neutron-deficient $^{44}Sc^{m}$ to neutron-excess ^{48}Sc.

II Experimental

Differential ranges were determined with 0.8, 3.0, 11.5, and 400 GeV incident protons. The experiments at 0.8 GeV were performed in line B of the Los Alamos Meson Physics Facility (LAMPF), those at 3.0 and 11.5 GeV in the internal beam of the Argonne National Laboratory zero gradient synchrotron (ZGS), and those at 400 GeV in the Neutrino Hall beam line at Fermilab. The irradiations were performed in either accelerator or beam line vacuum, or in the case of the 400 GeV irradiations, in an evacuated chamber.

The experiments involved the irradiation of thin UF_4 targets and the collection of the emitted fragments in a stack of thin (0.4-0.8 mg/cm^2) Mylar foils. The irradiation assemblies consisted of a target holder facing a cylindrical bed on which the catcher foils were mounted. The targets consisted of 0.1-0.3 mg/cm^2 UF_4 evaporated onto high-purity aluminum, and were inclined at 30° (ZGS) or 45° to the beam. The catcher foils were mounted so as to collect fragments emitted at 75°-105° to the beam, the mean recoil angle being $\sim$ 90°. The angular range was defined by a thick aluminum mask whose opening was cut along iso-theta lines.[16,17] The solid angle subtended by the catchers ranged from

0.34 sr at Fermilab to 0.66 sr at the ZGS. Fig. 1 shows an exploded view of the catcher assembly.

The irradiations were performed for periods ranging from ∿ 1h (ZGS) to ∿ 1 week (Fermilab). Following bombardment, the Mylar foils were dissolved and scandium separated by a previously described[1] radiochemical procedure from as many as 14 foils. The samples were assayed with Ge(Li) detectors and results obtained for $^{44}Sc^{m}$, ^{46}Sc, ^{47}Sc, and ^{48}Sc on the basis of the γ-rays emitted by these nuclides.[1] The differential ranges were obtained by extrapolation of the counting rates to end of bombardment and correction for chemical yield. The thickness of the catcher foils was determined gravimetrically and the results expressed as relative differential cross sections per unit thickness, $\frac{1}{\sigma_n}\left(\frac{d\sigma_n}{dx}\right)$ $(mg/cm^2)^{-1}$, where $d\sigma_n$ is the disintegration rate of a given nuclide in a foil of thickness dx and σ_n is the sum of all $d\sigma_n$ obtained in a given experiment.

Because of the relatively large solid angles intercepted by the catchers, the fragments struck the Mylar foils over a range of angles distributed about the normal direction. The effective catcher foil thickness is thus somewhat greater than the nominal value. The evaluation of this correction factor is complicated by the fact that the recoils originate at an extended source determined by the intersection of target and beam. The source profile was determined for each irradiation by cutting the target into 12-20 segments and assaying the ^{24}Na activity induced in the Al backing. The full widths at half-maximum in the x and y directions ranged from 0.2 and 0.4 cm, respectively, at Fermilab to

1.0 and 2.2 cm at LAMPF. These profiles, as well as the relevant geometric parameters, were used as input data in a code[17] that corrected the catcher thickness for the geometrical acceptance of recoils over all target-catcher points. The correction factors ranged from 2% at Fermilab to 7% at the ZGS. The effective target thickness was obtained by multiplying the nominal thickness by a similar correction factor and, in addition, taking into account the inclination of the target with respect to the catchers. The above code also permitted the evaluation of the solid angle subtended by the catcher foils as well as that of the mean recoil angle.

A number of experimental checks were performed in order to ensure the validity of the results. Enough Mylar foils were included in the catcher stacks to permit a determination of the activation of possible trans-scandium impurities in the Mylar. It was found that the activity of Sc in the farthest foils, which were well beyond the range of the fragments, was less than 0.1% of the peak activity indicating the absence of a measurable activation blank. Of greater importance was the possible contribution from impurities in the Al target backing or from the activation of various components of the irradiation assembly by the beam halo or by secondaries produced upstream. Target backing activation was essentially eliminated by use of 99.999% pure Al. The contribution of externally produced Sc fragments was minimized by use of plastic materials in the construction of the irradiation assembly wherever practical. Occasional blank runs indicated that the contribution of Sc fragments from extraneous sources was less than 0.5%. In the course of the

experiment it became apparent that the results of a given irradiation provided a clear internal indication of significant activation problems arising from the occasional beam focusing and steering difficulties that were encountered. The interaction of energetic hadrons with iron, the most likely extraneous source of fragments, leads to the formation of low-energy neutron deficient Sc nuclides by spallation but does not produce significant amounts of ^{48}Sc. The occurrence of these problems could thus be detected by the observation of an aberrant $^{44}Sc^{m}$ differential range coupled with a normal ^{48}Sc spectrum. The occasional experiments that showed this unusual isotopic difference were discarded.

The possible effect of the finite target thickness on the differential ranges was investigated at 11.5 GeV in experiments in which the results obtained with 0.1 and 0.3 mg/cm^2 thick targets were compared. As there were no significant differences between the two sets of differential ranges it was concluded that scattering effects could be neglected for targets in the above thickness range.

III Results

A. Differential Ranges

The results of typical differential range experiments are shown as histograms in Fig. 2. The indicated uncertainties were obtained by combining those in the Mylar foil thickness and uniformity (3%), chemical yield determination (2%), and correction for path length dispersion (1%) with the statistical error. The overall uncertainties typically ranged from $\sim$ 4% near the peak of the differential range to $\sim$ 50% for

the last foil showing activity above background, except for ^{46}Sc whose long half-life led to larger statistical errors. The histograms shown in Fig. 2 have not been corrected for loss of resolution resulting from the finite catcher thickness. A resolution correction was applied to each foil on the bases of the differential cross sections of the immediately adjacent foils in the manner described in previous studies.[11,12,18] This correction transformed the original range histogram into a "point" distribution, corresponding to the differential cross sections at the effective midpoints of the catchers. The resolution correction decreased the width of the narrow differential ranges, obtained at 0.8 GeV, by 10-15%, while the broader curves obtained at the higher energies decreased in width by only about 3%. The correction to the mean ranges is much smaller, decreasing in magnitude from $\sim$ 4% at 0.8 GeV to $<$ 1% at 400 GeV.

In order to facilitate the combination of replicate results as well as the transformation from range to energy spectra, the corrected differential ranges were curve-fitted by use of a non-linear regression analysis code.[17] First, a Gaussian carrier function was fitted to the "point" distribution. Once the best fit was obtained, the carrier function was subtracted from the data points. The resulting residual was in turn fitted with a polynomial function and the latter was added to the carrier function. This process was iterated until the minimum χ^2 value was obtained. The curves in Fig. 2 represent the results of this process. Note that the curves generally do not pass through the midpoints of the histograms but through the effective midpoints, the

difference being particularly noticeable in the steepest regions of the curves.

The average ranges were obtained from the corrected data after the application of a further correction for energy loss in the UF_4 target. It was assumed that, on the average, the fragments traversed half the effective target thickness. This thickness was converted to the Mylar equivalent on the basis of the relative stopping powers of Mylar and UF_4 for scandium fragments.[19] Typical energy losses in the target ranged from $\sim$ 5% for 20 MeV fragments to 1% for 150 MeV fragments. These losses are equivalent to $\sim$ 0.04 mg/cm^2 additional Mylar. The average ranges are summarized in Table I. Replicate determinations of the differential ranges were performed at all energies and the results are weighted averages. The tabulated errors are the larger of the standard deviation in the mean and the estimated uncertainty in the individual determinations.

It should be noted that all the Sc nuclides excepting ^{47}Sc are independently formed. The latter is also produced by the β^- decay of ^{47}Ca. However, charge dispersion systematics[1] indicate that for the present experimental conditions the contribution of ^{47}Ca to the ^{47}Sc differential range is < 5%. The experimental results consequently refer to Z=21 fragments in all cases.

B. Energy spectra

The corrected differential ranges were converted to energy spectra by use of the range-energy table of Northcliffe and Schilling (NS).[19]

A small correction, amounting to < 1% for all but the lowest energy fragments, was applied to account for the difference between the tabulated[19] path lengths and the experimentally determined projected ranges. The magnitude of this correction was obtained from the work of Lindhard, Scharff and Schiøtt.[20] The spectra obtained for $^{44}Sc^{m}$ and ^{47}Sc are displayed in Figs. 3 and 4, respectively. The points represent the transformed "point" differential ranges. The results of both experiments performed at each energy are included. The error bars incorporate an estimated 5% uncertainty in the range-energy relation. The curves were obtained from the corresponding fitted range curves generated with the average values of the Gaussian and polynomial parameters obtained in replicate experiments. It is seen that the curves in general represent an excellent fit to the data points. The spectra obtained for ^{46}Sc and ^{48}Sc are virtually indistinguishable from the ^{47}Sc spectra.

The spectra obtained for 0.8 GeV protons, while narrow, show the presence of a definite low-energy tail. It is not clear whether this is a real feature or the result of scattering in the target. As indicated above, the effect of target thickness was investigated at 11.5 GeV and showed that the spectra were independent of thickness. However, the broader spectra obtained at this energy would have precluded the observation of a scattering effect at the level shown by the 0.8 GeV data.

Hubert et al.[21] have recently compiled a new range-energy table for 2.5-12 MeV/nucleon ions on the basis of some recent stopping power measurements.[22] This table indicates that for the highest energy Sc fragments of present interest, the NS compilation underestimates the

fragment energy by $\sim$ 4%. This result applies to Sc stopping in carbon, the medium closest in composition to Mylar for which a direct comparison is possible. It should be noted that Hubert et al.[21] normalize their ranges to those of NS at 2.5 MeV/nucleon. Since most of the observed Sc fragments have energies below this value we are unable to draw more than the qualitative conclusion that our reported kinetic energies may be systematically low.

The spectra may be characterized by the mean energy $\langle T_R \rangle$ and by the full width at half-maximum. These quantities are tabulated in Table I. The listed uncertainties were obtained in the same manner as those in the ranges. We have not folded in the uncertainty in the range-energy relation since it doesn't enter to a significant extent in a comparison of the various Sc fragments or in the dependence of these quantities on bombarding energy.

If the small contribution to the fragment energy of the transverse component of velocity of the moving system is neglected, the tabulated values of $\langle T_R \rangle$ are comparable to those derived from thick-target recoil studies. The latter yield mean ranges in uranium, which may be directly converted to $\langle T_R \rangle$ values by use of the NS range-energy tables and the application of various corrections. Scheidemann and Porile[1] obtained results of this type for essentially the same energy range as that covered in the present study. Their values of $\langle T_R \rangle$ are uniformly higher than the present results, the discrepancy ranging from $\sim$ 30% at 0.8 GeV, where the fragments have the highest mean energies, to $\sim$ 10% at the higher energies where the mean recoil energies are relatively low.

Since Hubert et al.[21] claim that the NS range-energy table is most erroneous for light stopping media, the above discrepancies may constitute a reflection of this fact. On the other hand, Ravn[23] performed a similar thick-target experiment at 18 GeV and his derived energies are some 10% lower than the present values at 11.5 GeV and closely comparable to those obtained with 400 GeV protons.

IV Discussion

A. Variation of the spectra with energy and isotopic mass

The results displayed in Figs. 3 and 4 show that the spectra of both neutron-excess and neutron-deficient Sc fragments vary in a similar way with bombarding energy. At 0.8 GeV the spectra are fairly narrow and peak at moderately high energies, $\sim$ 90 MeV. With increasing bombarding energy the peaks shift to lower values and the curves become increasingly broad. These trends are quantified in Fig. 5, which shows the dependence of the mean fragment energies, the widths of the spectra, and the percentage of high ($T_R \geq 110$ MeV) and low-energy ($T_R \leq 60$ MeV) fragments on proton energy. The mean energies are essentially independent of fragment mass. The values of $\langle T_R \rangle$ decrease by some 45% between 0.8 and 11.5 GeV and by an additional 15% between 11.5 and 400 GeV. The widths of the spectra show the opposite dependence on bombarding energy, increasing sharply between 0.8 and 11.5 GeV, and then more gradually at higher energies. While isotopic differences in the widths are minor, it does appear that the $^{44}Sc^{m}$ spectrum is uniformly broader than those of the neutron-excess nuclides.

The variation with proton energy of low and high-energy recoils provides yet a more detailed picture of the effects of isotopic mass and bombarding energy on the spectra. As already apparent in Figs. 3 and 4, the fraction of low-energy recoils increases rapidly up to 11.5 GeV and more slowly thereafter. Fig. 5 indicates, in addition, that there is a significant isotopic difference between $^{44}Sc^{m}$ and the neutron-excess fragments at 0.8 GeV, where the fraction of low-energy recoils, as defined above, is twice as large in the $^{44}Sc^{m}$ spectrum. This isotopic effect vanishes by 3 GeV. The trends discussed above suggest that the fraction of high-energy recoils should decrease with increasing proton energy. This is indeed the case above 3 GeV. However, between 0.8 and 3 GeV the fraction of these fragments either increases or remains unchanged. A significant isotopic difference is once again noted at 0.8 GeV, where the $^{44}Sc^{m}$ spectrum has a greater fraction of high-energy fragments than the other spectra.

The spectra obtained at 0.8 GeV are indicative of a two-body breakup process such as highly asymmetric fission. Scheidemann and Porile[1] compared the mean momenta of fragments emitted in the interaction of 0.5-0.7 GeV protons with ^{238}U with the predictions of the liquid drop model of overlapping spheroids.[5] The results for Sc nuclides were found to be consistent with the fission of a moderately light nucleus, ^{203}Bi. Confirmatory evidence for this production model comes from the results of studies of coincident fission fragments. Remsberg et al. measured the energies and masses of fission fragments emitted in the interaction of ^{238}U [ref. 24] and ^{209}Bi [ref. 25] with 2.9 GeV protons. Although the statistics were too low to permit the observation of fragments

having A < 60 from the ^{238}U target, results were reported for A=40-50 fragments from ^{209}Bi. The mean kinetic energy of fragments in this mass range is $\sim$ 75 MeV and the full width is $\sim$ 30 MeV. These values are quite close to those obtained in the present work at 0.8 GeV. This agreement confirms the supposition[1] that the formation of Sc fragments at this energy results from the breakup of a nucleus some 30-40 mass units lighter than the target. The difference in bombarding energies should have only a minor effect on this conclusion.

Remsberg et al.[25] compared the mass-yield curve for fission fragments from ^{209}Bi with that obtained radiochemically for the interaction of lead with 3 GeV protons.[26,27] The comparison showed that for products in the A=40-50 mass region, fission accounts for only about 10% of the observed cross section. The present results support this conclusion. The decrease in the mean fragment energy and the concomitant broadening which occurs with increasing proton energy are an indication that the relative contribution of binary fission decreases. It appears, instead, that at the higher energies these products are the result of deep spallation. This process involves the breakup of the struck nucleus through a number of decay channels, ranging from nucleon to fragment emission. Since the breakup process does not involve the formation of two massive fragments, the kinetic energies are lower than they are in fission and the spectra are broader. In view of the fact that this process favors the formation of neutron-deficient products it is not surprising to find that the $^{44}Sc^{m}$ spectra are somewhat broader than those of the neutron-excess products.

Cumming and Bächmann[28] have derived from general considerations of

random addition of vectors and momentum conservation an equation that gives a semi-quantitative indication of a spallation or deep spallation mechanism. These workers related the mean kinetic energy of the observed product $\langle T_F \rangle$ to the mean energy of the emitted particles $\langle t_i \rangle$ by the relation

$$\langle t_i \rangle = \langle T_F \rangle A_T/(A_T - A_F) \quad (1)$$

where A_T and A_F are the mass numbers of target and product, respectively. The values of $\langle t_i \rangle$ were derived for a variety of target-product combinations and found to increase slowly with the mass difference between target and product. A short extrapolation of Cumming's systematics[28] indicates that the formation of ^{47}Sc by deep spallation of uranium requires that $\langle t_i \rangle$ be approximately 63 MeV. The values of $\langle t_i \rangle$ derived from the experimental values of $\langle T_F \rangle$ in Table I decrease from 104 MeV at 0.8 GeV to 72 MeV at 11.5 GeV, and to 63 MeV at 400 GeV. The formation of Sc nuclides from ^{238}U at high energies is, from this viewpoint, consistent with a deep spallation process.

B. Comparison with statistical model of fragment emission

Poskanzer and collaborators[13,14] have fitted the spectra of fragments emitted in the interaction of high-energy hadrons with heavy elements with a single Maxwell-Boltzmann distribution resulting from a moving thermal source. Their formulation incorporates in a simple way an adjustable Coulomb barrier, whose purpose is to reproduce the energies at which the peaks occur, and barrier smearing, whose function is to match the widths of the peaks. In addition, two-body breakup kinematics are included to correct for recoil. This approach has successfully systematized a large body of data with a relatively small number of parameters which vary in a fairly systematic way over the mass range of observed fragments. While the physical significance of all of these parameters is not com-

pletely clear and while, furthermore, the underlying assumption of an equilibrated emitting nucleus is questionable, the agreement between the model and the data is nonetheless impressive.

It is of interest to see how well this model can fit the spectra of Sc fragments at the various proton energies of interest. As discussed above, the spectra change in a gradual but marked way with bombarding energy in a manner that suggests a change in reaction mechanism. These data thus offer a somewhat different challenge to the model than the more usual test, in which the spectra of a broad range of fragments emitted in the interaction of a particular target with protons of a given energy are fitted. Furthermore, the avoidance of a low-energy cut-off permits the model to be tested at energies that lie below the threshold of counter experiments.

The specific equation proposed by Westfall et al.[13] for the double differential cross section for the emission of fragments in the moving system is

$$\frac{d^2\sigma}{dT_R' d\Omega'} = \frac{1}{2\Delta} \int_{k=<k>-\Delta}^{<k>+\Delta} \frac{\nu\sigma}{2(\pi\tau)^{3/2}} (\nu T_R' - kB)^{1/2} \quad x$$

$$\exp[-(\nu T_R' - kB)/\tau]\, dk,$$

$$(\nu T_R' > kB), \qquad (\Delta \leq <k>) \tag{2}$$

where ν is the correction for recoil and is given by

$$\nu = A_E/(A_E - A_F) , \tag{3}$$

A_E being the mass number of the emitting nucleus and A_F that of the fragment. The classical barrier B, corresponding to spheres in contact is given by

$$B = \frac{Z_F(Z_E - Z_F)\, e^2}{1.44\,[A_F^{1/3} + (A_E - A_F)^{1/3}]} \quad \text{MeV.} \tag{4}$$

This barrier is reduced by the factor k, which can range from $\langle k \rangle - \Delta$ to $\langle k \rangle + \Delta$, $\langle k \rangle$ being the mean reduction factor and Δ the smearing parameter. The nuclear temperature or slope parameter is designated τ. Eq. (2) is readily transformed to the laboratory system by the relation

$$\frac{d^2\sigma}{dT_R d\Omega} = \left(\frac{T_R}{T_R'}\right)^{1/2} \frac{d^2\sigma}{dT_R' d\Omega'} \tag{5}$$

and, for fragments emitted at 90°, the lab energy T_R is related to T_R' by

$$T_R' = T_R + A_R\, v_{||}^2/2 \tag{6}$$

where $v_{||}$ is the velocity of the moving system.

It is assumed in Eq. (2) that the probability of a given k value is uniformly distributed between $\langle k \rangle - \Delta$ and $\langle k \rangle + \Delta$. Westfall et al.[13] report that when this distribution is applied to the evaluation of the spectra of fragments emitted from uranium, it results in a shoulder on the high-energy

side of the peak which is not present in the data. These workers suggest that a Gaussian distribution of k values with a full width of 0.68 times 2Δ might give better agreement. We have verified that this is indeed the case and have used the following distribution function for k:

$$P(k) = \frac{0.691}{\Delta} \exp -(1.5\,[(k-\langle k\rangle)/\Delta]^2) \tag{7}$$

Incorporating the additional fact that our results are presented as fractional differential cross sections the function becomes

$$\frac{d\sigma_n/\sigma_n}{dT_R'} = \frac{1}{\int P(k)dk} \times \int P(k)\,\frac{\nu}{2(\pi\tau)^{3/2}}\,(\nu\,T_R' - kB)^{1/2} \times$$

$$\exp[-\,(\nu\,T_R' - kB)/\tau]\,dk \tag{8}$$

The above analysis was applied to the data for $^{44}Sc^m$ and ^{47}Sc, there being no significant difference between the spectra of ^{46}Sc, ^{48}Sc, and ^{47}Sc. Equation (8) was evaluated for a range of values of the various parameters and the best ones obtained by means of a visual fit. It was found that the value of τ determines the slope of the high-energy tails and, to a lesser extent, the width of the distribution. The smearing parameter Δ has the largest effect on the width and, in particular, determines the low-energy cutoff. The location of the peak in the spectra is determined by the effective barrier $\langle k\rangle B$. As indicated by Eq. (4), a given value of $\langle k\rangle B$ can be obtained by a combination of different values of $\langle k\rangle$ and (Z_E, A_E), a small value of $\langle k\rangle$ being nearly equivalent to a large value of Z_E and vice-versa.

In spite of this ambiguity these two parameters must be considered separately since the recoil correction factor ν depends only on A_E while Δ is limited by the value of $\langle k \rangle$. We have used the following procedure to obtain the values of $\langle k \rangle$ and (Z_E, A_E). At 0.8 GeV Monte Carlo cascade calculations are sufficiently reliable to permit an estimate of the identity of the average residual nucleus resulting from high-energy transfers. If it is assumed that this nucleus is the emitting system it then becomes possible to determine $\langle k \rangle$. A detailed examination of the Metropolis cascades[29] indicates that ^{233}Pa is a reasonable choice at this energy. When the barrier is evaluated by means of Eq. (4) the result for $\langle k \rangle$ is 0.55 for $^{44}Sc^{m}$ and 0.60 for ^{47}Sc. If we assume that the value of $\langle k \rangle$ is independent of the identity of the emitting nucleus it becomes possible to identify the latter at the higher energies on the basis of the 0.8 GeV $\langle k \rangle$ values. The ^{47}Sc results are consistent with the emitting nuclei ^{194}Pt at 3 GeV, ^{143}Pm at 11.5 GeV, and ^{137}Pr at 400 GeV, while the $^{44}Sc^{m}$ data require somewhat lighter emitters. In arriving at these results we have assumed that the ratio of the number of ejected neutrons and protons is approximately two, as indicated by the cascade calculations.[29] Finally, in order to evaluate the spectra in the laboratory system the velocity of the emitting nucleus must be known, as indicated in Eq. (6). Since this velocity is much smaller than that acquired by the fragment in the breakup step, its effect is almost negligible and the values derived from thick-target recoil studies[1] are perfectly adequate.

The results of this analysis are depicted in Figs. 6 and 7. It can

be seen that the calculation adequately reproduces the gradual broadening and shift to lower peak energies observed with increasing proton energy. The exponential tails are in some instances not very well defined in the data but the statistical uncertainties are large and the number of data points in this region is rather small. The biggest discrepancy occurs at low fragment energies where the calculation invariable underestimates the differential cross sections. This discrepancy is most severe at low proton energies where the narrowness of the spectra requires relatively low values of the smearing parameter. These low values of Δ preclude the reproduction of the low-energy tails. Recall, however, that scattering effects may enhance the magnitude of these tails. In their recent study of fragment emission Westfall et al.[13] reported spectra of fragments as massive as Ar. Their low-energy cutoff for the ^{238}U target was about 40 MeV. Figs. 6 and 7 indicate that the discrepancies between the data and the model occur below this energy and so were not observed in their work.

An attempt was made to improve the agreement between the model and experiment by use of a pre-exponential term in T_R' rather than $(T_R')^{1/2}$. This choice corresponds to emission from the nuclear surface rather than from the volume.[30] However, as already reported by Westfall et al.,[13] the presence of the Coulomb barrier renders the function insensitive to the form of the pre-exponential term.

The parameters resulting in the best fits to the data are plotted as a function of bombarding energy in Fig. 8. The temperature increases be-

tween 0.8 and 3 GeV to a value of 19±2 MeV and then becomes invariant. At 0.8 GeV there is a substantial isotope effect, the neutron-excess fragments displaying a much lower temperature. This result is not surprising if these fragments are indeed formed in highly asymmetric binary fission at this energy. It is well known[31] that neutron-excess fission fragments require lower deposition energies than neutron-deficient fission fragments of comparable mass. Since the nuclear temperature is a measure of the deposition energy the observed result follows. Our result at 3 GeV and above is somewhat higher than the value of 14 MeV reported by Westfall et al.[13] for Ar fragments.

The values of Δ increase markedly with bombarding energy up to 11.5 GeV, reflecting the observed broadening, and then level off at the limit defined by $\langle k \rangle$. There does not appear to be a significant isotope effect. Westfall et al.[13] report a Δ of 0.3 for Ar fragments, in reasonably good agreement with the present results.

The effective barrier displays the opposite dependence on bombarding energy, decreasing sharply up to 11.5 GeV and then only slightly thereafter. While $\langle k \rangle_B$ for ^{47}Sc is uniformly larger than that for $^{44}Sc^m$, the difference lies within the respective uncertainties. As discussed above, the decrease in $\langle k \rangle_B$ can be related to the decrease in the mass of the emitting nucleus. While the actual masses of these nuclides as derived from the analysis should not be taken too seriously it is nonetheless clear that, within the context of a two-body breakup process, the mass loss via other decay channels must increase very markedly between 0.8 and 11.5 GeV. Under these circumstances the difference

between two-body breakup and deep spallation largely disappears since extensive mass dissipation is, in fact, the salient feature of this process.

V Conclusions

The differential ranges of $^{44}Sc^{m}$, ^{46}Sc, ^{47}Sc, and ^{48}Sc emitted at 90° to the beam in the interaction of ^{238}U with 0.8, 3.0, 11.5, and 400 GeV protons have been measured and transformed to the corresponding energy spectra. All the spectra broaden with increasing proton energy and the peaks shift to lower energies, the changes being most pronounced between 0.8 and 11.5 GeV. Isotopic effects are virtually absent except at 0.8 GeV, where a broader spectrum is obtained for $^{44}Sc^{m}$ than for the neutron-excess fragments. The results are consistent with highly asymmetric binary fission of a moderately light nucleus at 0.8 GeV but suggest an increasing contribution of deep spallation at the higher energies.

The spectra have been compared with a statistical model of fragment emission[13,14] and reasonable fits were obtained except in the region of low fragment energies, where the model underestimates the relative number of fragments. Although considerable ambiguity in the identity of the emitting nucleus exists, it is clear that mass dissipation becomes increasingly extensive with increasing proton energy and must amount to close to half the target mass at the highest bombarding energy. Under these circumstances, the distinction between two-body breakup and deep spallation becomes largely semantic.

We wish to acknowledge the cooperation and assistance of E. P. Steinberg and S. B. Kaufman with the ZGS irradiations, and that of B. J. Dropesky with the LAMPF experiments. The Fermilab experiments were performed in conjunction with similar measurements by a University of Chicago group and we wish to acknowledge the cooperation of N. Sugarman and R. A. Johns. We are grateful to the Plastic Products and Resins Department of Du Pont for providing us with the thin Mylar foil. This work was financially supported by the U.S. Department of Energy.

References

1. Ø Scheidemann and N. T. Porile, Phys. Rev. C14, 1534 (1976).
2. K. Beg and N. T. Porile, Phys. Rev. C3, 1631 (1971).
3. S. B. Kaufman and M. W. Weisfield, Phys. Rev. C11, 1258 (1975).
4. S. B. Kaufman, E. P. Steinberg, and M. W. Weisfield, Phys. Rev. C18, 1349 (1978).
5. J. R. Nix and W. J. Swiatecki, Nucl. Phys. 71, 1 (1965).
6. D. R. Fortney and N. T. Porile, Phys. Lett. 76B, 553 (1978).
7. S. Biswas and N. T. Porile, Phys. Rev. C (in press).
8. W. Busza, in "High-Energy Physics and Nuclear Structure- 1975", Santa Fe and Los Alamos, ed. by D. E. Nagle et al. (A.I.P., New York, 1975).
9. G. Berlad, A. Dar, and G. Eilam, Phys. Rev. D13, 161 (1976).
10. Meng Ta-chung, Phys. Rev. D15, 197 (1977). Meng Ta-chung and E. Moeller, Phys. Rev. Lett. 41, 1352 (1978).
11. K. Bächmann and J. B. Cumming, Phys. Rev. C5, 210 (1972).
12. N. T. Porile, S. Pandian, H. Klonk, C. R. Rudy, and E. P. Steinberg, Phys. Rev. C19, 1832 (1979).
13. G. D. Westfall, R. G. Sextro, A. M. Poskanzer, A. M. Zebelman, G. W. Butler, and E. K. Hyde, Phys. Rev. C17, 1368 (1978).
14. A. M. Poskanzer, G. W. Butler, and E. K. Hyde, Phys. Rev. C3, 882 (1971).
15. J. Gosset, H. H. Gutbrod, W. G. Meyer, A. M. Poskanzer, A. Sandoval, R. Stock, and G. D. Westfall, Phys. Rev. C16, 629 (1977).
16. C. R. Rudy, N. T. Porile, and S. B. Kaufman, Nucl. Instrum. Methods 138, 19 (1976).

17. D. R. Fortney, Ph. D. Thesis, Purdue University, May, 1979 (unpublished).

18. V. P. Crespo, J. B. Cumming, and A. M. Poskanzer, Phys. Rev. 174, 1455 (1968).

19. L. C. Northcliffe and R. F. Schilling, Nucl. Data A7, 233 (1970).

20. J. Lindhard, M. Scharff and M. E. Schiøtt, Kgl. Danske Videnskab. Selskab, Mat. -Fys. Medd. 33, No.14 (1963).

21. F. Hubert, A. Fleury, R. Bimbot, and D. Gardés, CEN-IPN Report CENBG 7821 - IPN-RC-7807, 1978 (unpublished).

22. R. Bimbot, S. Della Negra, D. Gardés, H. Gauvin, A. Fleury, and F. Hubert, Nucl. Instrum. Methods 153, 161 (1978).

23. H. Ravn, J. Inorg. Nucl. Chem. 31, 1883 (1969).

24. L. P. Remsberg, F. Plasil, J. B. Cumming, and M. L. Perlman, Phys. Rev. 187, 1597 (1969).

25. L. P. Remsberg, F. Plasil, J. B. Cumming, and M. L. Perlman, Phys. Rev. C1, 265 (1970).

26. G. Friedlander, in "Physics and Chemistry of Fission" (International Atomic Energy Agency, Vienna, 1965), Vol. 2, p. 265.

27. N. T. Porile, Phys. Rev. 148, 1235 (1966).

28. J. B. Cumming and K. Bächmann, Phys. Rev. C6, 1362 (1972).

29. N. Metropolis, R. Bivins, M. Storm, J. M. Miller, G. Friedlander and A. Turkevich, Phys. Rev. 110, 1490 (1958).

30. A. S. Goldhaber, Phys. Rev. C17, 2243 (1978).

31. J. J. Hogan and N. Sugarman, Phys. Rev. 182, 1210 (1969).

Table I. Quantities derived from differential ranges of Sc fragments emitted at 90° to the beam.

T_p (GeV)	Nuclide	<R> (mg/cm^2)	$<T_R>$ (MeV)	FWHM (MeV)
0.8	$^{44}Sc^m$	3.12±.06	84.7±1.6[a]	27.4±0.6
	^{46}Sc	2.90±.12	77.0±3.2	18.1±1.4
	^{47}Sc	3.10±.06	83.1±1.6	24.5±0.3
	^{48}Sc	3.10±.06	82.8±1.6	25.4±0.4
3.0	$^{44}Sc^m$	2.76±.08	73.5±2.1	52.5±0.7
	^{46}Sc	2.58±.13	66.3±3.3	74.6±1.0
	^{47}Sc	2.75±.08	74.2±2.1	49.6±0.7
	^{48}Sc	2.71±.06	71.5±1.6	52.2±0.7
11.5	$^{44}Sc^m$	2.25±.04	57.8±1.0	72.4±1.0
	^{46}Sc	2.28±.09	57.1±2.2	71.9±1.0
	^{47}Sc	2.29±.04	58.2±1.0	68.5±1.0
	^{48}Sc	2.30±.04	57.8±1.0	67.2±1.0
400	$^{44}Sc^m$	2.06±.05	49.2±1.2	84.5±1.2
	^{46}Sc	2.14±.08	51.3±1.9	79.6±1.5
	^{47}Sc	2.11±.04	50.6±1.0	76.9±1.2
	^{48}Sc	2.14±.04	50.4±1.0	79.4±1.2

a. The errors do not include an estimated 5% uncertainty in the range-energy relation.

Figures

Fig. 1. Exploded view of Mylar stack.

Fig. 2. Differential ranges of Sc fragments emitted at 90° in the interaction of ^{238}U with 0.8 - 400 GeV protons. The solid histograms show the results of typical experiments and the dashed lines give an indication of the experimental uncertainties. The curves are the results of a fit described in the text. The arrows surmounting the curves correspond to the mean ranges. The results have not been corrected for energy loss in the target.

Fig. 3. Energy spectra of $^{44}Sc^{m}$ fragments emitted at 90° in the interaction of ^{238}U with 0.8 - 400 GeV protons. The curves through the data points were obtained from the fits to the differential ranges as described in the text. The spectra are arbitrarily displaced from each other.

Fig. 4. Energy spectra of ^{47}Sc fragments. See Fig. 3 for details.

Fig. 5. Dependence on proton energy of the mean kinetic energies (top panel), full-widths-at-half-maximum (middle) and percent of high-energy ($T_R \geq 110$ MeV, solid curves) and low-energy ($T_R \leq 60$ MeV, dashed curves) fragments. The symbols represent the various Sc nuclides: o, $^{44}Sc^{m}$; ▲, ^{46}Sc; ●, ^{47}Sc; ■, ^{48}Sc. The results for ^{46}Sc have been omitted from the bottom panel because of the large statistical uncertainties.

Fig. 6. Comparison of experimental spectra of $^{44}Sc^{m}$ (points) with statistical fragment emission calculation described in text (curves).

Fig. 7. Comparison of experimental spectra of ^{47}Sc with calculation. See Fig. 6 for details.

Fig. 8. Energy dependence of Maxwellian parameters for $^{44}Sc^{m}$ (open points) and ^{47}Sc (closed).

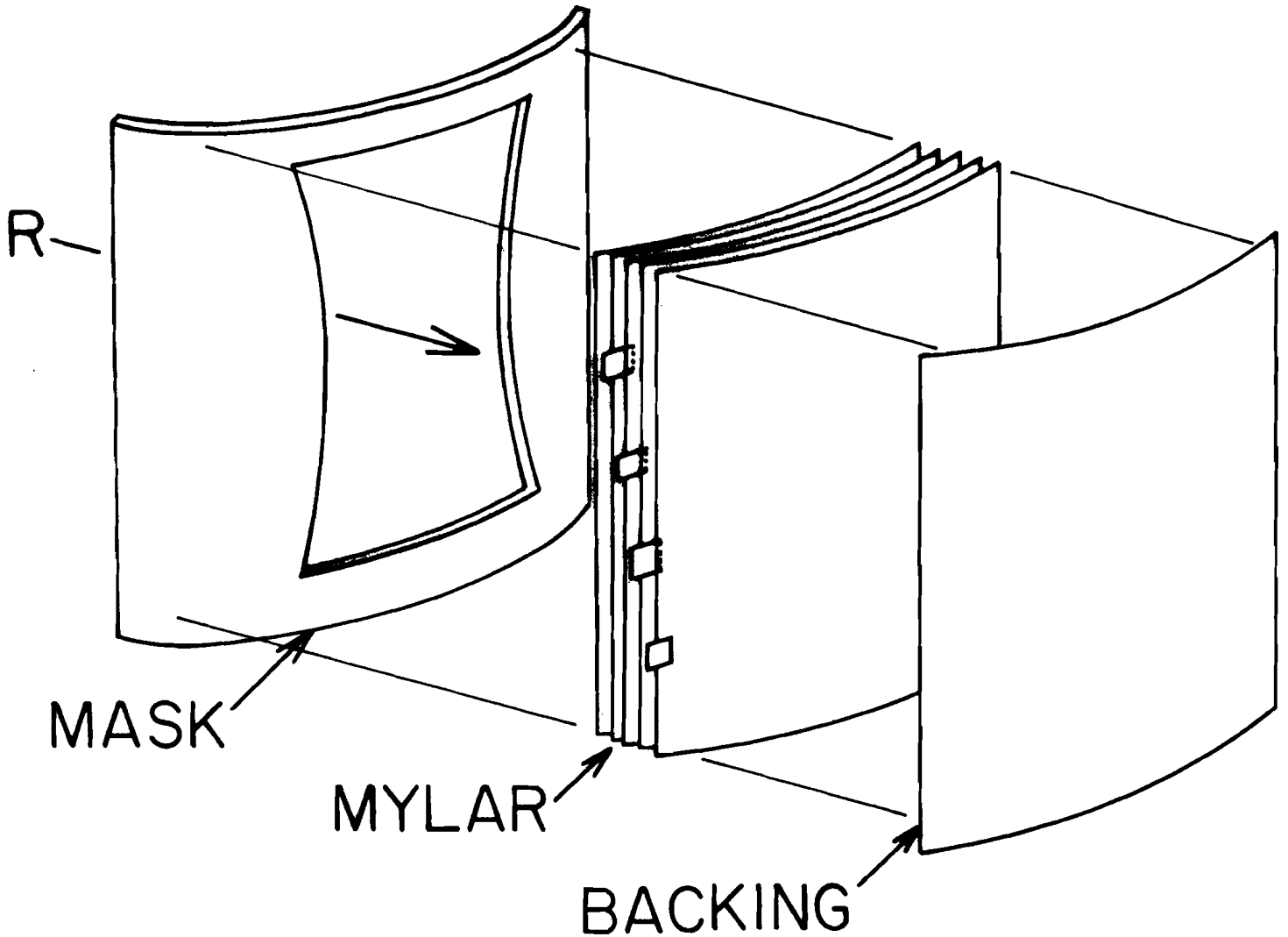

Fig 1

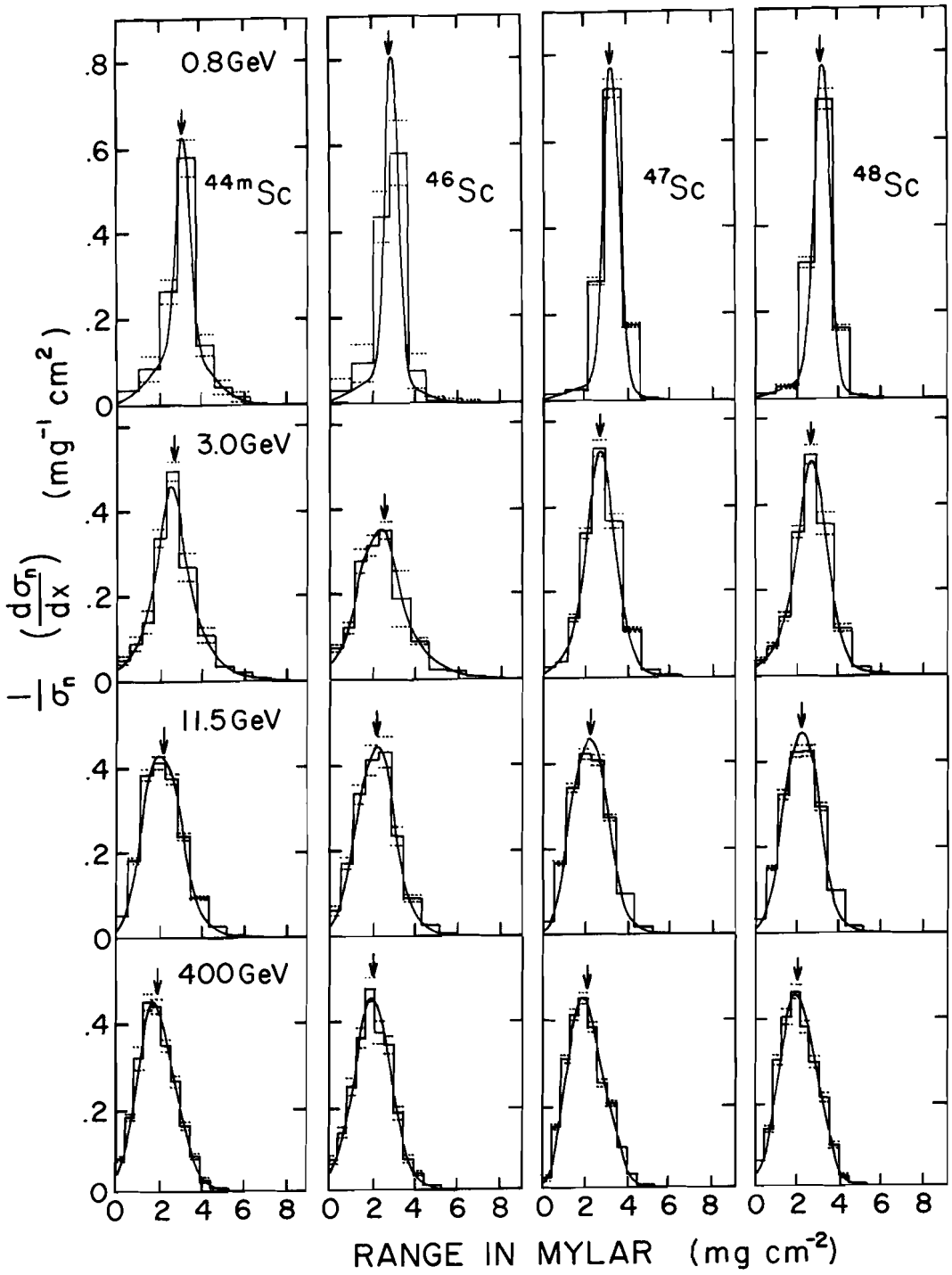
0.8GeV
3.0GeV
11.5GeV
400GeV
44mSc
46Sc
47Sc
48Sc
$\frac{1}{\sigma_n}\left(\frac{d\sigma_n}{dx}\right)$ (mg^{-1} cm^2)
RANGE IN MYLAR (mg cm^{-2})

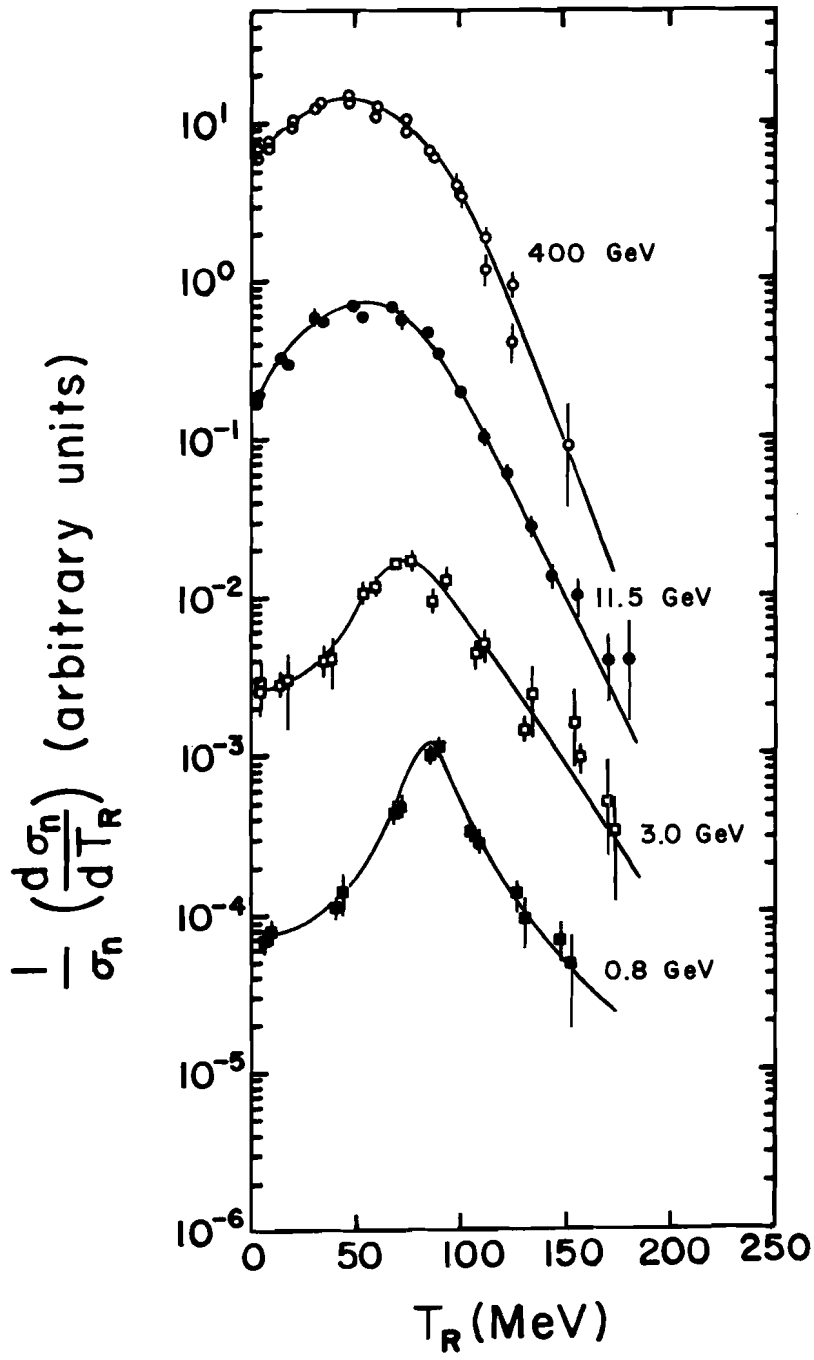
$\frac{1}{\sigma_n}\left(\frac{d\sigma_n}{dT_R}\right)$ (arbitrary units)
10^1
10^0
10^{-1}
10^{-2}
10^{-3}
10^{-4}
10^{-5}
10^{-6}
400 GeV
11.5 GeV
3.0 GeV
0.8 GeV
0
50
100
150
200
250
T_R (MeV)

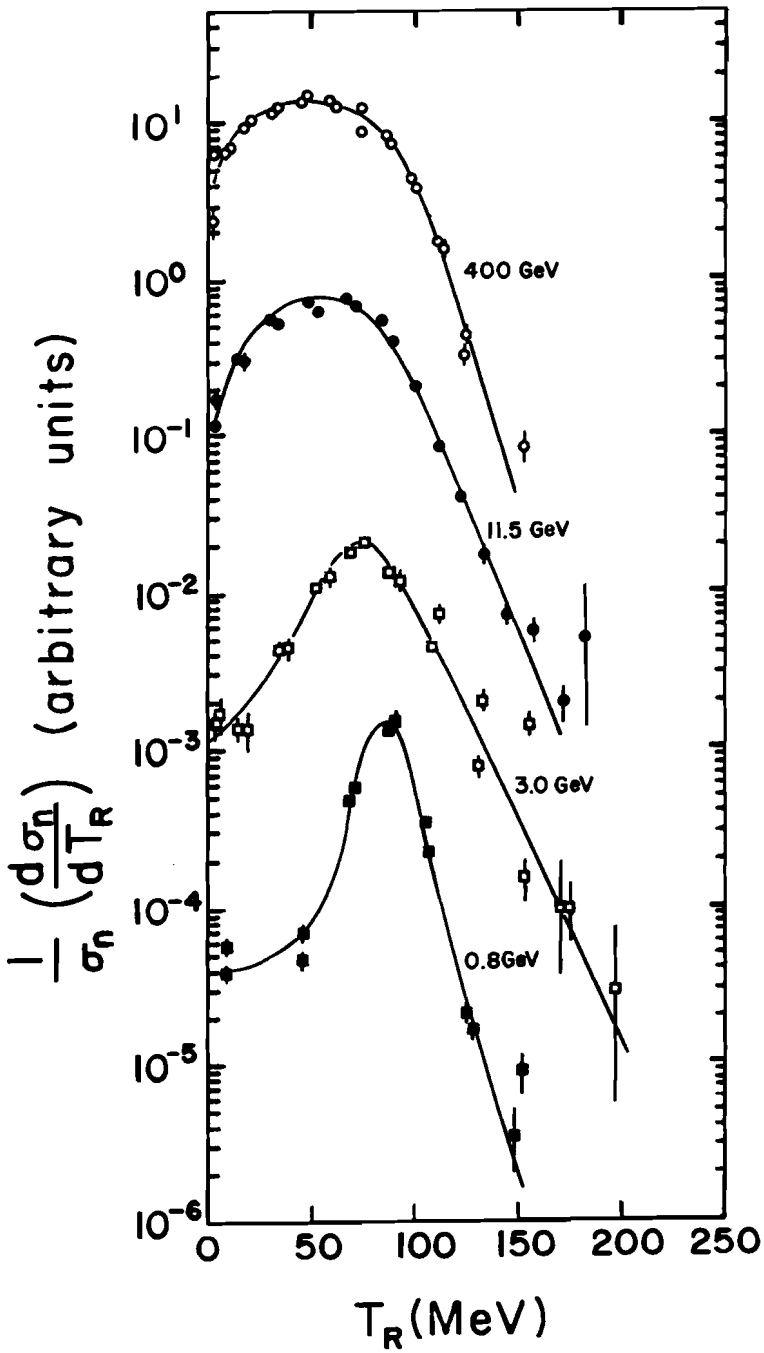
$\frac{1}{\sigma_n}\left(\frac{d\sigma_n}{dT_R}\right)$ (arbitrary units)
10^1
10^0
10^{-1}
10^{-2}
10^{-3}
10^{-4}
10^{-5}
10^{-6}
400 GeV
11.5 GeV
3.0 GeV
0.8GeV
0
50
100
150
200
250
T_R(MeV)

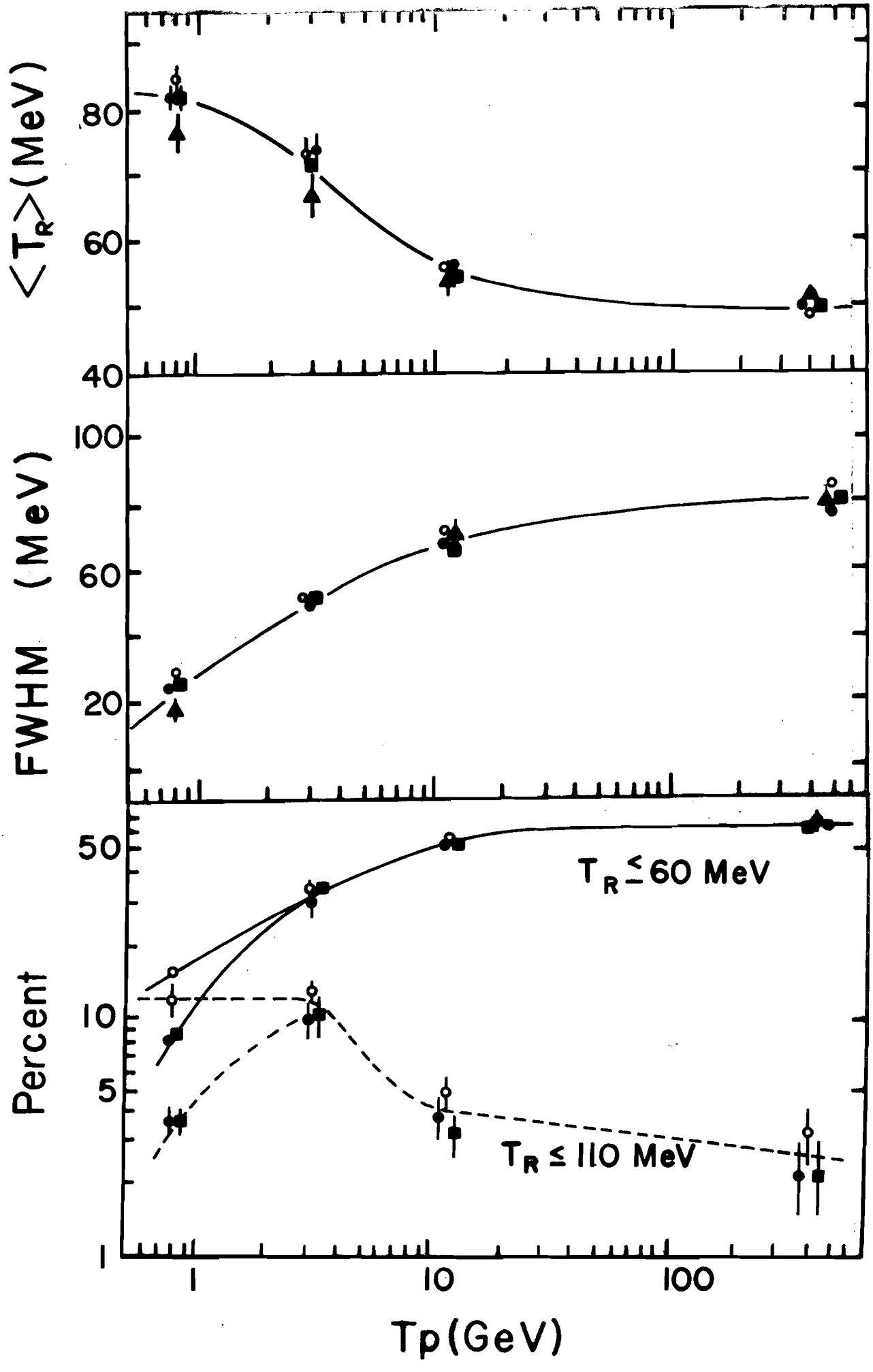
$\langle T_R \rangle$ (MeV)
80
60
40
FWHM (MeV)
100
60
20
Percent
50
10
5
1
$T_R \leq 60$ MeV
$T_R \leq 110$ MeV
1
10
100
Tp(GeV)

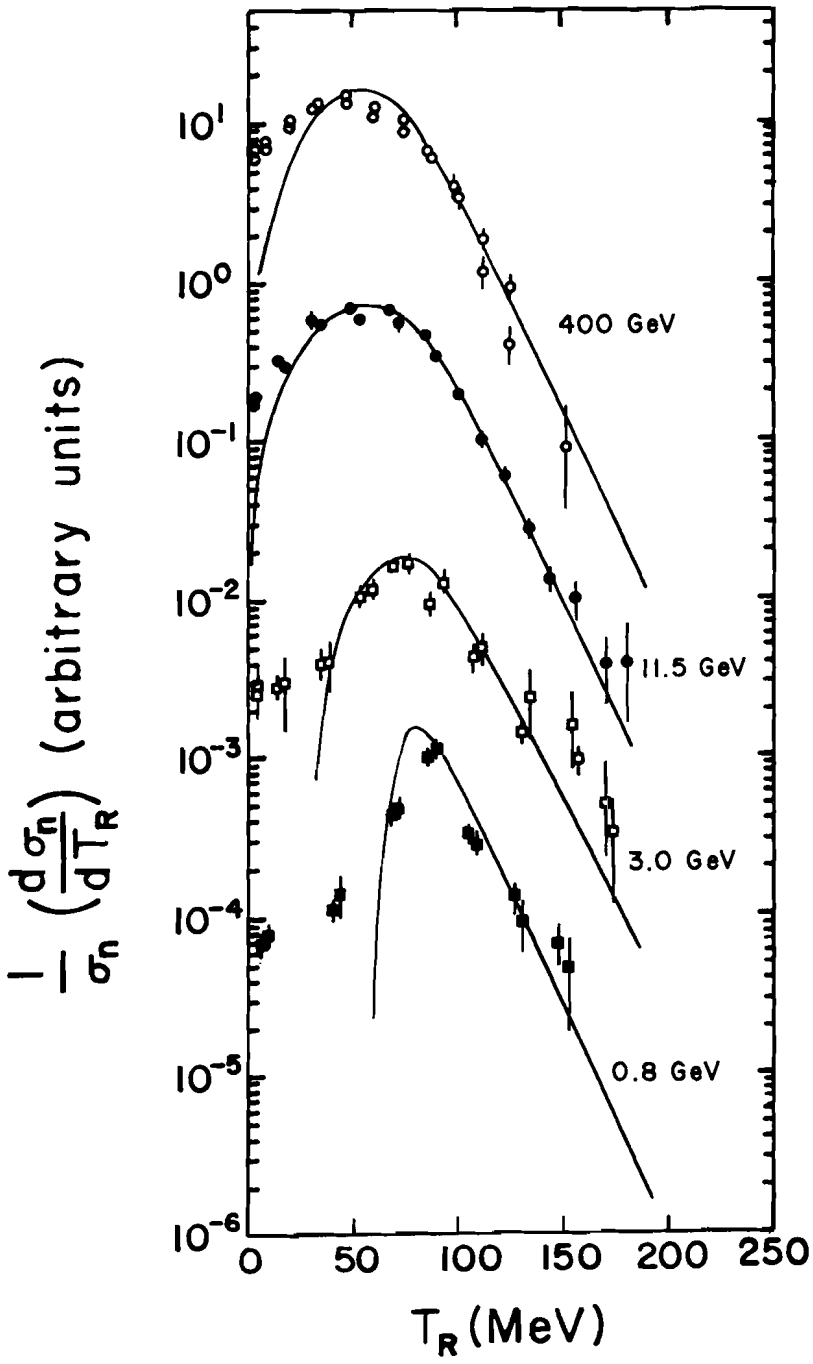
$\frac{1}{\sigma_n}\left(\frac{d\sigma_n}{dT_R}\right)$ (arbitrary units)
10^{1}
10^{0}
10^{-1}
10^{-2}
10^{-3}
10^{-4}
10^{-5}
10^{-6}
400 GeV
11.5 GeV
3.0 GeV
0.8 GeV
0
50
100
150
200
250
T_R (MeV)

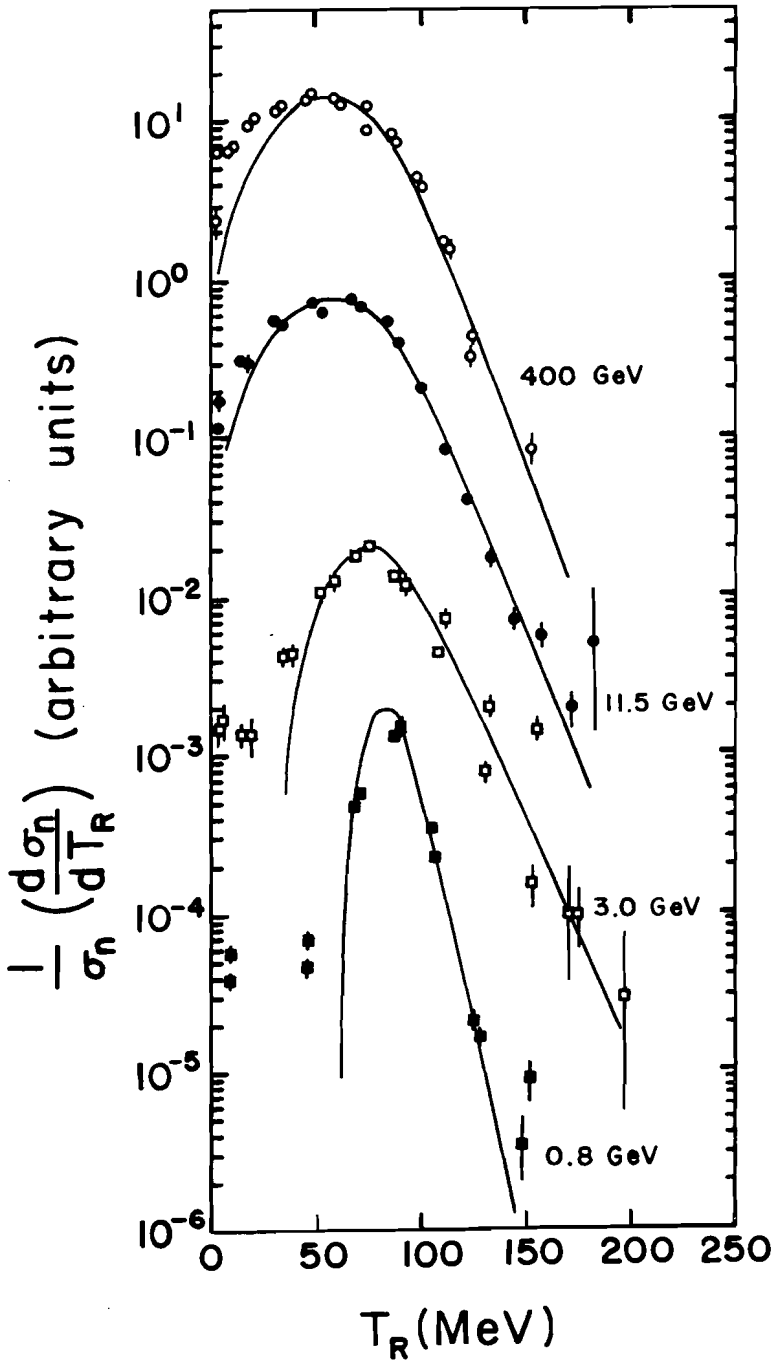
$\frac{1}{\sigma_n}\left(\frac{d\sigma_n}{dT_R}\right)$ (arbitrary units)
10^{1}
10^{0}
10^{-1}
10^{-2}
10^{-3}
10^{-4}
10^{-5}
10^{-6}
400 GeV
11.5 GeV
3.0 GeV
0.8 GeV
0
50
100
150
200
250
T_R(MeV)

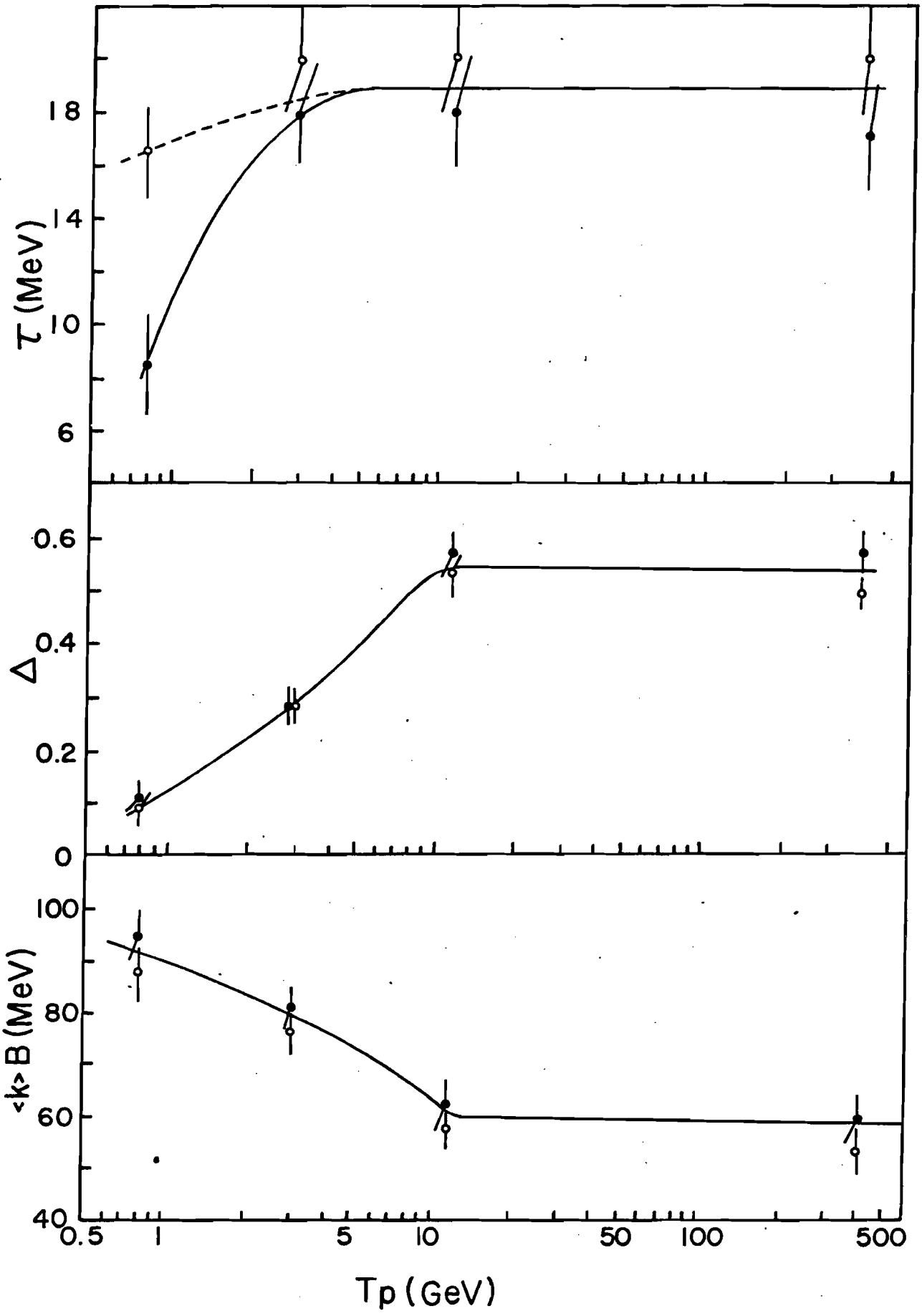
18
14
10
6
τ (MeV)
0.6
0.4
0.2
0
Δ
100
80
60
40
<k> B (MeV)
0.5
1
5
10
50
100
500
Tp (GeV)